EFFECTS OF RENEWABLE ENERGY UNSTABLE SOURCE TO HYDROGEN PRODUCTION: SAFETY CONSIDERATIONS

Melideo, D.[1], Liponi, A[1], Rastelli, D.[2], Rizza, M.E.[2], Ferrari, L.[1], Desideri, U.[1]
[1] DESTEC, Univeristà di Pisa, Largo Lucio Lazzarino, 56122, Pisa, Italy, daniele.melideo@unipi.it
[2] McPhy Energy Italia Srl, Via Ayrton Senna n. 22, San Miniato (Pisa), 56028, Italy

ABSTRACT

Hydrogen is considered a promising energy carrier for a sustainable future when it is produced by utilizing renewable energy. Nowadays, less than 4% of hydrogen production is based on electrolysis processes. Each component of a hydrogen energy system needs to be optimized to increase the operation time and system efficiency. Only in this way hydrogen produced by electrolysis processes can be competitive with the conventional fossil energy sources.

As conventional electrolysers are designed for operation at fixed process conditions, the implementation of fluctuating and highly intermittent renewable energy is challenging. Alkaline water electrolysis is a key technology for large-scale hydrogen production powered by renewable energy. At low power availability, conventional alkaline water electrolysers show a limited part-load range due to an increased gas impurity. Explosive mixtures of hydrogen and oxygen must be prevented; thus, a safety shutdown is performed when reaching specific gas contamination.

The University of Pisa is setting up a dedicated laboratory, including a 40-kW commercial alkaline electrolyser: the focus of the study is to analyze the safety of the electrolyser, together with its performance and the real energy efficiency, analyzing its operational data collected under different operating conditions affected by the unstable energy supply.

1. INTRODUCTION

Hydrogen is expected to play an important role as an energy carrier for the future of energy systems, especially when it is produced with renewable energy [1–5]. Only 4% of current hydrogen production is done using electrolysis due to the high cost of the process; the rest is obtained from fossil fuels (i.e. 48% via steam reforming of natural gas, 30% via petroleum fraction, and 18% via coal gasification) [6], [7], releasing about 830 million tons of carbon dioxide per year, according to the recent report prepared by the International Energy Agency (IEA) [8] for the G20 meeting in Japan.

To reduce CO_2 emissions and to become independent of fossil energy carriers, the share of hydrogen produced using renewable power sources needs to be increased significantly in the next few decades. Therefore, water electrolysis is a key technology for splitting water into hydrogen and oxygen by using renewable energy. Since solar and wind energy distribution is the most widespread, they are the preferred renewable power sources for hydrogen production; coupling water electrolysis with renewable energy can bring to particular advantages, since the exceeding electrical energy produced can be stored in hydrogen, balancing the discrepancy between energy demand and production [9–11]. The main issue with the use of renewable energy is the unsteady distributed and intermittent local availability [10].

There are three different technologies for water electrolysis: alkaline water electrolysis (AEL), proton exchange membrane (or polymer electrolyte membrane) electrolysis (PEM), and solid oxide electrolysis (SOEL) [12–14]; the first two are at low temperature and a well-established technology, while the last one adopts an high temperature technology and it is still in a development stage [15]. Often, PEM systems are preferred for dynamic operation due to the short start-up time and a broad load flexibility

range (e.g. automatic application), while alkaline water electrolysis are mainly used for static application [16], [17]. Alkaline water electrolysis uses concentrated lye as an electrolyte and requires a gas-impermeable separator to prevent the product gases from mixing. The electrodes consist of non-noble metals like nickel with an electrocatalytic coating.

When an alkaline water electrolysis is coupled with fluctuating renewable energy (e.g. solar or wind farms), it has to be analyzed how a dynamic system will affect the whole operation: alkaline water electrolysis must to be optimized for dynamic operation when used together with renewable energy sourced in order to guarantee safety and high efficiency.

The University of Pisa, in particular the Department of Energy, Systems, Territory and Construction Engineering, is setting up a laboratory to measure the hydrogen quality and safety of an alkaline electrolyser when coupled with an un-steady power supply (e.g. due to a renewable source input).

2. ALKALINE WATER ELECTROLYSIS

Alkaline water electrolysis is used to split water into the gases hydrogen and oxygen using electric energy. The principle of the alkaline water electrolysis is quite simple. Oxygen and hydrogen are separated from the water when the direct current is applied to the water, as shown in the following equations:

$$\textit{Cathode:}\quad 2\,H_2O_{(l)} + 2e^- \rightarrow H_{2(g)} + 2\,OH^-_{(aq)} \qquad (1)$$

$$\textit{Anode:}\quad 2\,OH^-_{(aq)} \rightarrow 0.5\,O_{2(g)} + H_2O_{(l)} + 2e^- \qquad (2)$$

$$\textit{Overall reaction:}\ H_2O_{(l)} \rightarrow H_{2(g)} + 0.5\,O_{2(g)} \qquad (3)$$

At the cathode, water molecules are reduced by electrons to hydrogen and negatively charged hydroxide ions. At the anode, hydroxide ions are oxidized to oxygen and water while releasing electrons. Overall, a water molecule reacts to hydrogen and oxygen in the ratio of 2:1.

2.1 Cell design

The design of the electrolysis stack depends on the manufacturer; however, some general similarities can be observed. Usually alkaline electrolysers contain demi water solution and 25%–30% of potassium hydroxide (KOH); for small size alkaline electrolysers, KOH is sometimes replaced by sodium hydroxide (NaOH). The liquid electrolyte allows ions to be transported between the electrodes and is not consumed in the chemical reaction, but is periodically supplied depending on the losses in the system.

During the electrolysis, hydrogen is produced in cathodic chambers, while oxygen is produced in the anodic chambers, as represented in Figure 1.

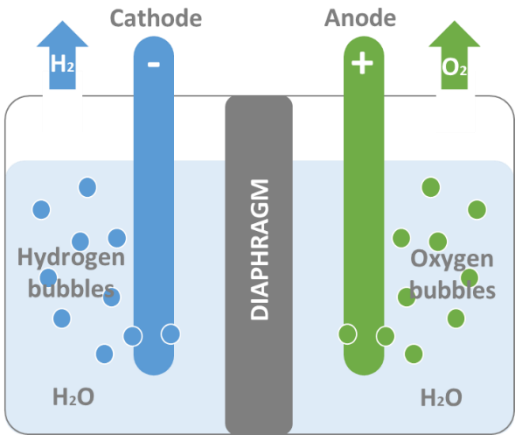

Figure 1. Water electrolysis schematic diagram

The main function of the diaphragm, placed between the two electrolytic chambers is to avoid the mixture of the two gases.

2.2 Gas purity

Gas purity is an important criterion of alkaline water electrolysis. The produced hydrogen typically has a purity higher than 99.8 vol.% (without additional purification), [18]. Hydrogen has a very broad flammability range: 4% to 75% concentration in air and 4% to 94% in oxygen; therefore, keeping air or oxygen from mixing with hydrogen inside confined spaces is very important. Also, it requires only 0.02 millijoules of energy to ignite the hydrogen–air mixture, which is less than 7 percent of the energy needed to ignite natural gas. Technical safety limits for an emergency shutdown of the whole electrolyser system are at a level of 2 vol.% [19], [12]; that limit is also required by technical standard [20]: the electrolysis process must be stopped at the fulfilment of 2% of H_2 mixed with O_2 (i.e. 50% of lower explosive limit at atmospheric pressure) and 1.6% of O_2 mixed with H_2 (i.e. 98.4% of H_2, which is 4.4 percentage points above the upper explosive limit of hydrogen at atmospheric pressure) regardless to temperature and pressure values.

The hydrogen generated by an electrolyser contains a certain amount of oxygen (OTH), whilst the oxygen generated contains a certain amount of hydrogen (HTO). By measuring these impurities, it is possible to determine with sufficient accuracy the purity of the gases generated by the alkaline electrolyser, as well as the amount of hydrogen and oxygen escaping through the diaphragms and electrolyte pathways. HTO in relation to temperature and for an operating pressure of 25 bar, and in relation to pressure and for an operating temperature of 65° C are studied in [18] and reported in Figure 2 (left hand side and right hand side respectively).

The results show an increase in HTO as the current decreases. This is due to a reduction in the process gas flow rate and, therefore, to an increase in the time the gases remain in the electrolysis cells. The hydrogen molecules produced at the electrodes join up more slowly to form bubbles and, consequently, the molecules are held inside the cell for a longer period of time, thereby contributing to the increase in the hydrogen diffusion rate through the diaphragms. Likewise, the HTO trend is exponential with the decrease in current, being more significant at high operating temperatures and pressures. This exponential trend is associated with a considerable decrease in the production of hydrogen at low currents due to the parasitic currents through the electrolyser stack. The left graph in Figure 2 shows an increase in HTO as the temperature increases, with a quasi-linear trend for each current. For example, for the 120 A current, the HTO is shown to be 80% greater at 65° C (0.27 vol.%) compared to 35° C (0.15 vol.%). Making this same comparison for 40 A, the HTO is 115% greater at 65° C (1.72 vol.%) compared to 35° C (0.8 vol.%). The temperature increase in the electrolysis stack leads to an increase

in the diffusion rate for the small gas bubbles through the diaphragms. When the process temperature increases, the thermal energy available in the system also increases and the particles, including the gases, increase their mobility.

Pressure is an even greater determining factor for HTO than temperature. As shown in the right graph in Figure 2, as the pressure increases, the HTO value for each current level increased quasi-proportionally. For example, when the operating pressure is 5 bar, the HTO value for 40 A is 0.36 vol.%, whilst for a pressure of 25 bar and the same current level, it is approximately 4.8 times greater, that is 1.72 vol.%. For 120 A, the HTO is 4.5 times greater at 25 bar (0.27 vol.%) compared to 5 bar (0.06 vol.%). The decrease in the volume of the gas bubbles generated in the electrolysis module is practically inversely proportional to the pressure increase. This decrease in the size of the bubbles leads to a greater migration of hydrogen through the electrolyte pathways and diaphragm pores.

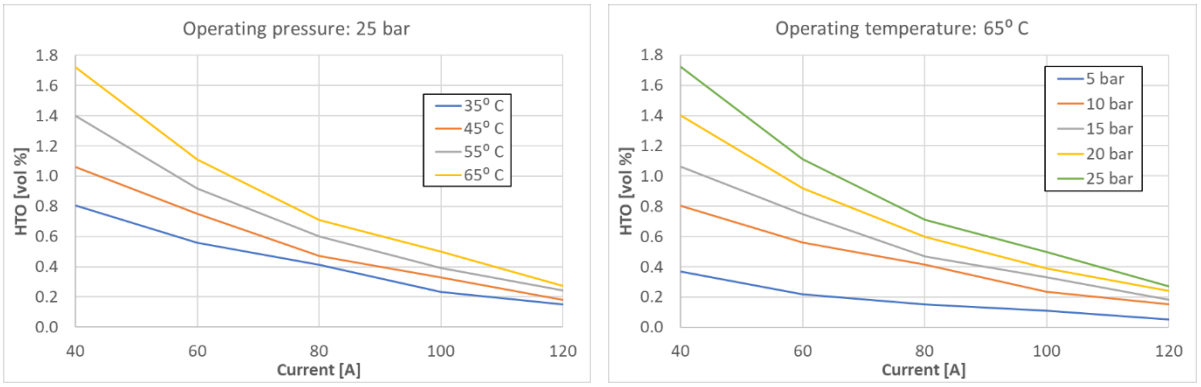

Figure 2. Hydrogen transferred to the oxygen flow (HTO) in relation to temperature and for an operating pressure of 25 bar (left), and in relation to pressure and for an operating temperature of 65° C (right). The current, temperature and pressure ranges are the ones analysed in the experiment performed in [18].

OTH trends with current, temperature and pressure are equivalent to the HTO ones analysed above. However, comparing the HTO values obtained with those for the OTH for each current, temperature and pressure level, it can be seen that the HTO is 10-30 times greater than the OTH (for small size alkaline electrolysers HTO is usually 3-7 times greater than the OTH). Such high differences are attributable to the fact that the hydrogen molecules, in addition to being lighter than the other elements, are also smaller and therefore have a greater fugacity and diffusivity through the electrolyte pathways and stack cell diaphragms, compared to oxygen.

The analysis of the influence of current, temperature and pressure on the HTO and OTH has revealed a number of interesting points, such as the best operating conditions to minimise HTO and OTH are basically those in which the electrolyser is operating at a low pressures and high currents.

Anodic gas impurities for alkaline water electrolysis are also experimentally determined for different operation mode in [21]: the experiments confirm the lower is the pressure level, the lower is the gas impurities.

3. MAIN CURRENT SAFETY AND TECHNICAL REGULATIONS FOR ELECTROLYSIS AND RELEVANT HAZARDS IDENTIFICATION

All the devices relevant for hydrogen production must to be complied with ATEX directives [6]; the directive defines the essential health and safety requirements and conformity assessment procedures, to be applied before products are placed on the EU market. In particular, such directive covers equipment

and protective systems intended for use in potentially explosive atmospheres. The explosive atmosphere is defined as a mixture of air with dangerous substances in the form of gases, vapour, mist or dust; after ignition has occurred, combustion spreads to the entire unburned mixture.

Other CE marking Directives relevant for hydrogen production are the Pressure Equipment Directive, (PED) [22], the Machinery Directive [23], the Low Voltage Directive [24] and the Electromagnetic Compatibility Directive [25].

The relevant Standard document is the ISO 22734 (Hydrogen generators using water electrolysis) [20]: it defines the construction, safety, and performance requirements of modular or factory-matched hydrogen gas generators, using electrochemical reactions to electrolyse water to produce hydrogen.

Most recently, the Fuel Cell and Hydrogen Joint Undertaking (FCH JU), with the support of the European Hydrogen Safety Panel (EHSP), organized a workshop focused on the safety aspects of electrolysis technology. The main outcomes are reported in [26]. A typical cause of fires and explosion in alkaline chlorine electrolysis is the accidental creation and ignition of flammable gaseous mixtures (hydrogen-chlorine, hydrogen-air/oxygen).

The hazards generally addressed in electrolysis are small leaks due to imperfect sealing, impurities, cross-over (in particular oxygen into hydrogen product), accumulations of flammable inventory in the phase separators, and thermal stresses.

In the recent accident (2019) at the alkaline electrolyser in Gangneung, Korea, the introduction of hydrogen into the oxygen stream was not caused by membrane perforation, but gases cross-over under low power operating conditions [27]. Such cross-over was not detected and the typical catalytic oxygen removal system was not installed; an explosive mixture of hydrogen and oxygen formed in the hydrogen storage containers was ignited by an unknown source.

4. RENEWABLE POWER INPUT DATA

When coupled with renewable sources, the electrolyser is subject to a continuously fluctuating and intermittent power input. This leads the electrolyser to operate in part-load favouring gas impurities and the risk of reaching hazardous conditions.

In order to simulate the dynamic behaviour, a variable power data series reproducing the renewable power must be given as input to the electrolyser.

Annual 5-min wind speed data of a windy site were taken from the NREL Wind Prospector web site [28]. A site with an average wind speed of about 6 m/s at 100 m of height and a Weibull shape parameter of 2 was chosen since these are typical values for wind farms. The wind speed distribution of the site is shown in Figure 3 (left). The wind speed variation for a site is usually described using the Weibull distribution which is the probability density function of the wind speed. The integral of this function over a speed interval represents the probability of having a wind speed within that range. Therefore, the area under the whole curve is exactly 1.

Wind turbines manufacturers provide the power curve, a graph that describes the relationship between wind speed and turbine electrical power output. Wind turbines are usually designed to start running at a wind speed, called cut-in speed (v_{ci}), of around 3-5 m/s. The generated power reaches the rated power at rated speed. At cut-off speed (v_{co}), the turbine is stopped in order to avoid damaging the turbine and the surroundings.

From the wind speed data series, the wind power was calculated assuming a turbine power curve fitted and scaled from [29] and expressed as function of the wind speed (v_w) by:

$$P_{wt} = \begin{cases} 0\,, & v_w < v_{ci} \text{ or } v_w < v_{co} \\ (a_1 {v_w}^3 + a_2 {v_w}^2 + a_3 v_w + a_4)\, P_{wt,nom}, & v_{ci} \le v_w \le v_r \\ P_{wt,nom} & v_r \le v_w \le v_{co} \end{cases} \quad (4)$$

$$a_1 = -2.715\ 10^{-3}\ ({}^{m}/_{s})^{-3}, a_2 = 6.138\ 10^{-2}\ ({}^{m}/_{s})^{-2}, a_3 = -0.2950\ ({}^{m}/_{s})^{-1}, a_4 = 0.4318$$

where $P_{wt,nom}$ is the wind turbine rated power; v_{ci} = 3 m/s, v_{co} =25 m/s and v_r =11 m/s are the cut-in, cut-off and rated speeds, respectively.

The resulting wind power distribution for the chosen site is shown in Figure 3 (right). The y-axis indicates the percentage of time in a whole year in which the wind power is between each bar range. The red bar indicates the percentage of time in the year in which the turbine is stopped because the wind speed is below the cut-in speed or over the cut-off speed.

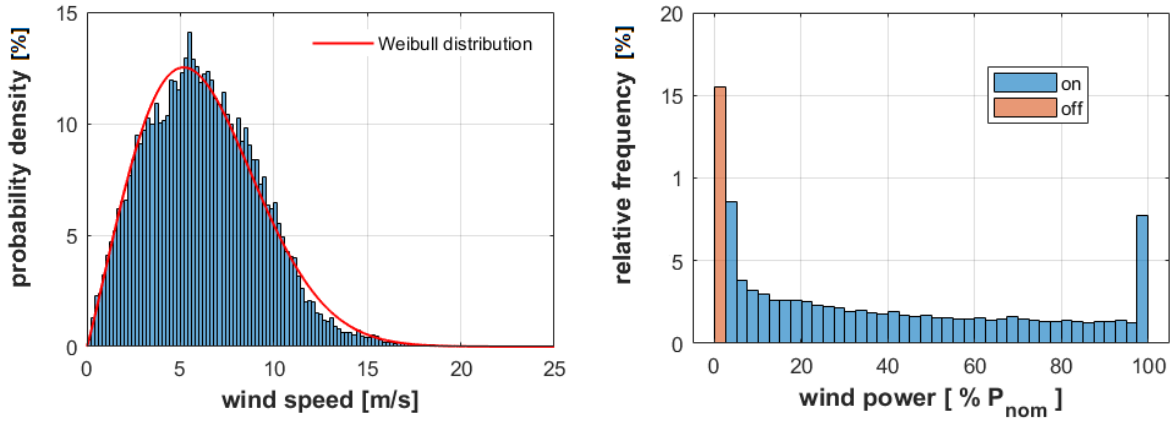

Figure 3. Wind speed distribution (left) and wind power distribution (right).

Similarly, 5-min Photovoltaic (PV) power series were taken from [30] and scaled so that the PV nominal power matched the electrolyser nominal power. A site located in the New York state (USA) was chosen since it is characterized by seasonal power variability (Figure 4). The PV power distribution of the selected data is shown in Figure 4 (right). The red bar indicates the percentage of time in the year in which the PV plant is not producing energy.

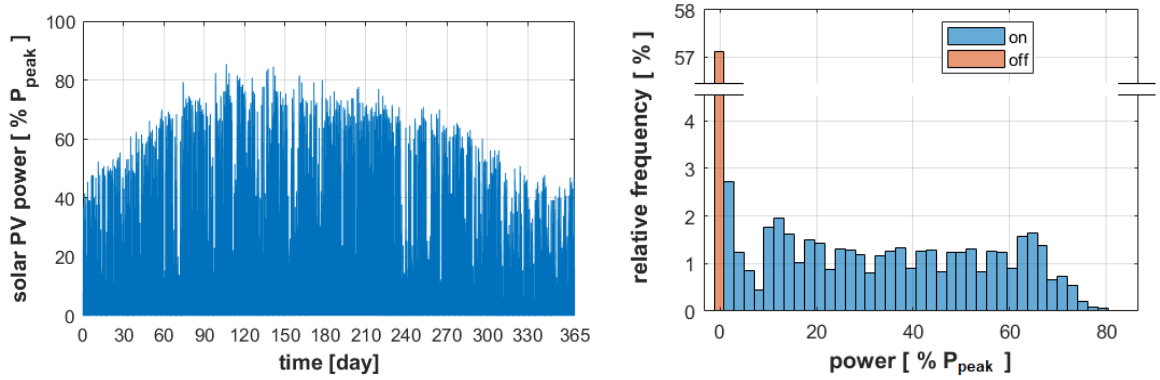

Figure 4. PV power vs time (left) and annual PV power distribution (right).

The wind and PV nominal power were set equal to the electrolyser nominal power. The electrolyser must work in a power range of 20-100% nominal power [31] to avoid safety issues. In fact, at lower powers, the lower currents lead to higher HTO and, consequently, to possible explosive atmospheres in the stack as shown in Figure 2. Therefore, the electrolyser power input was set equal to the renewable wind/PV power whenever the operating power limits are respected, and equal to zero (the electrolyser is shut down) if the renewable power is lower than the minimum allowed electrolyser power set at 20% of the nominal power. As a result, two electrolyser annual power input profiles were obtained respectively for the cases of wind and solar PV sources. As shown in Figure 5, the electrolyser power input follows the renewable power when possible and therefore, it is characterized by a high variability and frequent on-off.

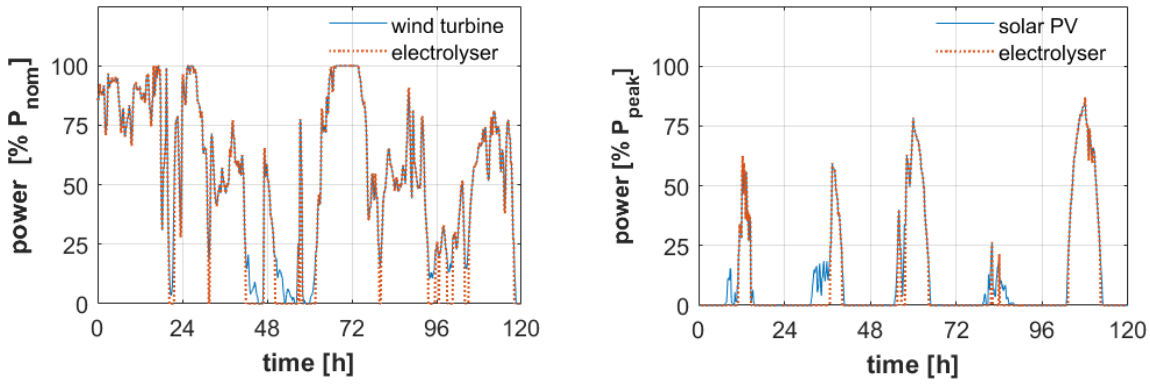

Figure 5. Wind/solar- and electrolyser- power vs time.

5. EXPERIMENTAL SET-UP

5.1 Hydrogen production

The selected hydrogen generation unit is a Piel M by McPhy; it is an alkaline electrolyser and it is designed to provide hydrogen at rated capacity up to 4.4 Nm³/h @ 2 barg (0.40 kg/h). The key features of the electrolyser are reported in Table 1.

Table 1. Electrolyser key features

Hydrogen production rate	4.4 Nm³/h
Oxygen production rate	2.2 Nm³/h
Hydrogen delivery pressure	2.0 barg
Hydrogen delivery quality	99.5% ± 0.3% dry basis

The electrolysis stacks produce hydrogen and oxygen based on an electrolytic process, using electricity as energy source. To produce 1 Nm³ of hydrogen, 3.55 kWh of electrical energy would be needed on a theoretical basis. However, due to the energy losses of the real process, at beginning of life at the stack level about 5.3 kWh of electric energy are required per Nm³ of H_2.

For safety reason, the unit can produce a hydrogen flowrate included in the range 25÷100 % of nominal flowrate. The unit includes all the equipment for a safe production of hydrogen at controlled pressure. In case of failure or lack of some service or utilities, a procedure of shutdown of the electrolyser starts

in a safe and controlled way: the current to the stack is set to zero and a procedure of depressurization is triggered.

The electrolyte, an aqueous alkaline solution with hydroxide compound, flows through the electrolysis stacks, where the electrolysis takes place. During the electrolysis, hydrogen appears in the cathodic chambers (hydrogen side of the separation membranes), as well as oxygen in the anodic chambers (oxygen side of the membranes). The purpose of the separation membranes placed between the electrolytic chambers is avoiding the mixture of the two gases. Immediately afterwards, the electrolyte containing hydrogen and the one containing oxygen flow toward the separator vessels. The temperature of the electrolyte containing hydrogen is monitored and a shutdown procedure is trigged when electrolyte temperature reaches 80 °C.

Inside the separation vessels, both the H_2 and O_2 bubbles are separated from the electrolyte. The volume of the generated hydrogen is twice the volume of the oxygen, in accordance to the theoretical equation (3). Both vessels are interconnected by a tube, in order to equalize the fluid level on both sides. The level is measured by two level sensors (one located in each vessel). The vessel liquid level is regulated to prevent emptying or overfilling.

The temperature of the electrolyte at the inlet of the electrolysis stacks is regulated by means of a thermal sensor and a temperature transmitter. The operative pressure of the electrolysis unit is set to 2 barg. The pressure transmitter controls the pressure inside the system by varying the power supply to the electrolysis stacks. When reaching a pressure over 2.5 barg the current is stopped and the plant enters in stand-by mode; when the pressure exceeds that limit a shutdown procedure will occur. There are two additional pressure switches to stop the system at very high pressure (i.e. 5 barg): two pressure safety valves release hydrogen or oxygen to the dedicated vent lines respectively.

5.2 Laboratory layout

The main components of the laboratory are reported in Figure 6. The laboratory is provided with two vents: the inlet vent is located close to the floor, while the outlet vent is located close to ceiling [32]; for guarantying the forced ventilation the outlet vent is equipped with a fan (ATEX [33] zone 2 certified) able to suck an adequate air change per hour, according to the electrolyser supplier requirements.

An ambient hydrogen sensor will be installed in the room for safety reason: the system is shut down when the safety limit of 0.4% of hydrogen in air is reached; this corresponds to the 10% of the lower flammable limit of H_2 in O_2 [20]. An important consideration is to understand where the sensor will be located, in order to increase the possibility to detect hydrogen, independently from the possible leak location, direction and orientation. For that reason, is important to predict the air flow inside the laboratory, considering the air circulation (due to the forced ventilation) and the presence of the obstacles. According to [34], the sensor has to be located not on a direct path of the airflow from the inlet vent to the outlet vent; a possible location is below the enclosure ceiling, but not in the proximity of obstacles (e.g. ceiling piping and lighting). An accurate prediction of hydrogen concentrations distribution requires an understanding of hydrogen behaviour inside the enclosure, which it might require the use of validated models; to address that issue, a possible Computational Fluid Dynamic (CFD) analysis of the hydrogen dispersion inside the laboratory is under consideration.

The electrolyser is fed with demineralized water. Before entering the electrolyser, the water temperature is controlled and measured (T_{IN}); the mass flow rate is also measured at the inlet of the electrolyser (MF_{IN}). A power control unit allows to modify the power input in order to simulate a fluctuating and intermittent power input due to the coupling with a renewable source (see paragraph 4).

The temperature and mass flow rate are measured at the exit of the electrolyser both at the hydrogen (T_{H2} and MF_{H2}) and oxygen (T_{O2} and MF_{O2}) lines.

The hydrogen stream will be analyzed with an on-line gas quality analyzer (H_2 quality) for quantifying the hydrogen quality, identifying the presence of impurities, in accordance with [35]. The presence of hydrogen in oxygen will be measured thanks to a sensor on the oxygen line.

The electrolyser gas line outlets are equipped with additional filter in order to preserve the integrity of the instrumentations: the H_2 and the O_2 are not completely dry, and may have some traces of NaOH.

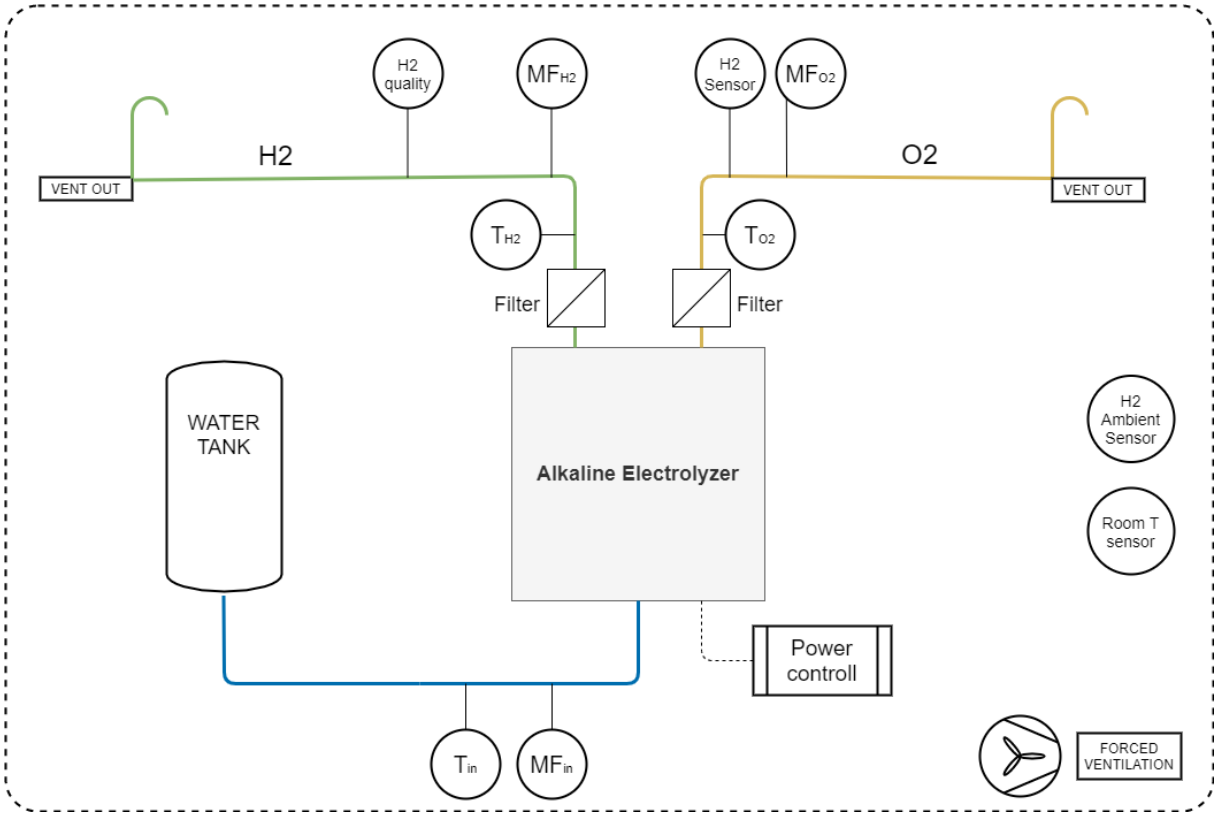

Figure 6. Scheme of the laboratory.

5.3 Future experimental activities

Firstly, polarization curve tests will be conducted in order to determine the change in the stack voltage with the variation in the supplied current under steady-state conditions at constant reference temperature and pressure. This test is carried out in galvanostatic mode by measuring the voltage imposing a continuous increase (ascending mode) / decrease (descending mode) of current density at a specific rate.

The electrolyser will then be tested under dynamic protocols consisting of potential sweeping with different with short holds to simulate alternating power operation. Furthermore, the electrolyser will be tested under a variable input power that simulates the renewable power assigned by the power control. During the tests, inlet and outlet flow rates, hydrogen impurities and HTO in the oxygen stream will be measured. The aim of the tests is to evaluate the effects of the dynamic operation on the hydrogen quality and possible safety issues.

6. CONCLUSION

At the Department of Energy, Systems, Territory and Construction Engineering of the University of Pisa, a dedicated laboratory is under development to measure the hydrogen quality of an alkaline

electrolyser when coupled with fluctuating renewable energy (e.g. solar or wind farms); also, the safety related issue will be analyzed.

In this paper the tentative laboratory layout is presented together with the planned future activities; mainly, two types of experiments are foreseen, using polarized curves to test the variation in the stack voltage and dynamic protocol to simulate alternating power operation. The first results are expected by the end of 2021.

REFERENCE

[1] Kerkhof A. Towards a hydrogen economy. Public Transp Int 2003;52:53. https://doi.org/10.1007/978-3-030-30908-4_4.

[2] Sherif SA, Barbir F, Veziroglu TN. Towards a Hydrogen Economy. Electr J 2005;18:62–76. https://doi.org/10.1016/j.tej.2005.06.003.

[3] Brandon NP, Kurban Z. Clean energy and the hydrogen economy. Philos Trans R Soc A Math Phys Eng Sci 2017;375. https://doi.org/10.1098/rsta.2016.0400.

[4] European Commission. Towards a hydrogen economy in Europe: a strategic outlook. Commun FROM Comm TO Eur Parliam Counc Eur Econ Soc Comm 2020.

[5] Tseng P, Lee J, Friley P. A hydrogen economy: Opportunities and challenges. Energy 2005;30:2703–20. https://doi.org/10.1016/j.energy.2004.07.015.

[6] Dixon RK, Li J, Wang MQ. Progress in hydrogen energy infrastructure development—addressing technical and institutional barriers, 2016, p. 323–43. https://doi.org/10.1016/B978-1-78242-362-1.00013-4.

[7] IRENA (International Renewable Energy Agency). Hydrogen From Renewable Power. 2018.

[8] IEA (International Energy Agency). The Future of Hydrogen. Rep Prep by IEA G20, Japan 2019. https://doi.org/10.1787/1e0514c4-en.

[9] Santos DMF, Sequeira CAC, Figueiredo JL. HYDROGEN PRODUCTION BY ALKALINE WATER ELECTROLYSIS. 2017 Int Conf Adv Comput Commun Informatics, ICACCI 2017 2017;2017-Janua:219–22. https://doi.org/10.1109/ICACCI.2017.8125843.

[10] Wang M, Wang Z, Gong X, Guo Z. The intensification technologies to water electrolysis for hydrogen production - A review. Renew Sustain Energy Rev 2014;29:573–88. https://doi.org/10.1016/j.rser.2013.08.090.

[11] Steilen M, Jörissen L. Hydrogen Conversion into Electricity and Thermal Energy by Fuel Cells: Use of H2-Systems and Batteries. Electrochem Energy Storage Renew Sources Grid Balanc 2015:143–58. https://doi.org/10.1016/B978-0-444-62616-5.00010-3.

[12] Schalenbach M, Zeradjanin AR, Kasian O, Cherevko S, Mayrhofer KJJ. A perspective on low-temperature water electrolysis - Challenges in alkaline and acidic technology. Int J Electrochem Sci 2018;13:1173–226. https://doi.org/10.20964/2018.02.26.

[13] Schmidt O, Gambhir A, Staffell I, Hawkes A, Nelson J, Few S. Future cost and performance of water electrolysis: An expert elicitation study. Int J Hydrogen Energy 2017;42:30470–92. https://doi.org/10.1016/j.ijhydene.2017.10.045.

[14] Carmo M, Fritz DL, Mergel J, Stolten D. A comprehensive review on PEM water electrolysis. Int J Hydrogen Energy 2013;38:4901–34. https://doi.org/10.1016/j.ijhydene.2013.01.151.

[15] David M, Ocampo-Martínez C, Sánchez-Peña R. Advances in alkaline water electrolyzers: A review. J Energy Storage 2019;23:392–403. https://doi.org/10.1016/j.est.2019.03.001.

[16] Tsoutsos T. Hybrid wind – hydrogen energy systems. Stand-Alone Hybrid Wind Energy Syst 2010.

[17] Shiva Kumar S, Himabindu V. Hydrogen production by PEM water electrolysis – A review. Mater Sci Energy Technol 2019;2:442–54. https://doi.org/10.1016/j.mset.2019.03.002.

[18] Ursúa A, San Martín I, Barrios EL, Sanchis P. Stand-alone operation of an alkaline water electrolyser fed by wind and photovoltaic systems. Int J Hydrogen Energy 2013;38:14952–67. https://doi.org/10.1016/j.ijhydene.2013.09.085.

[19] Haug P, Koj M, Turek T. Influence of process conditions on gas purity in alkaline water electrolysis. Int J Hydrogen Energy 2017;42:9406–18. https://doi.org/10.1016/j.ijhydene.2016.12.111.

[20] International Organization for Standardization (ISO). ISO 22734: Hydrogen generators using water electrolysis. 2019.

[21] Brauns J, Turek T. Alkaline water electrolysis powered by renewable energy: A review. Processes 2020;8. https://doi.org/10.3390/pr8020248.

[22] European Parliament and the Council of the European Union. Directive 2014/68/EU pressure equipment. Off J Eur Union 2014;93:164–259.

[23] European Parliament and the Council of the European Union. Machinery Directive 2006/42/EC.

Manuf Eng 1989;68:46–8. https://doi.org/10.1049/me:19890129.
[24] European Parliament and the Council of the European Union. Low Voltage Directive 2014/35/EU. Off J Eur Union 2014:357–74.
[25] European Parliament and the Council of the European Union. Electromagnetic compatibility Directive 2014/30/EU. Off J Eur Union 2014;29.3.2014:79–106.
[26] Azkarate I, Jordan T, Moretto P. Minutes of the FCH 2 JU Workshop on Safety of Electrolysis on 18 November 2020 2021:2–14.
[27] Kim, S. I.;Kim Y. Review: Hydrogen Tank Explosion in Gangneung, South Korea. Cent. Hydrog. Saf. Conf., 2019.
[28] Draxl C, Hodge BM, Clifton A, McCaa J. Overview and Meteorological Validation of the Wind Integration National Dataset Toolkit. 2015.
[29] Leitwind Technical Data Sheet n.d. https://www.leitwind.com/it/prodotti/fino-a-2mw/ltw90/23-0.html (accessed November 11, 2020).
[30] NREL. Solar Power Data for Integration Studies n.d. https://www.nrel.gov/grid/solar-power-data.html (accessed March 29, 2021).
[31] Schnuelle C, Wassermann T, Fuhrlaender D, Zondervan E. Dynamic hydrogen production from PV & wind direct electricity supply – Modeling and techno-economic assessment. Int J Hydrogen Energy 2020;45:29938–52. https://doi.org/10.1016/j.ijhydene.2020.08.044.
[32] NASA. Safety standard for hydgogen and hydrogen systems. Guidelines for Hydrogen System Design, Materials Selection, Operations, Storage, and Transportation. 1997.
[33] European Parliament and the Council of the European Union. Directive 2014/34/EU (ATEX) of the European Parlament and of the Council. Off J Eur Union 2014:309–56.
[34] Tchouvelev A V., Buttner WJ, Melideo D, Baraldi D, Angers B. Development of risk mitigation guidance for sensor placement inside mechanically ventilated enclosures – Phase 1. Int J Hydrogen Energy 2020;46:12439–54. https://doi.org/10.1016/j.ijhydene.2020.09.108.
[35] International Organization for Standardization (ISO). ISO 14687:2019 Hydrogen fuel quality — Product specification 2019.